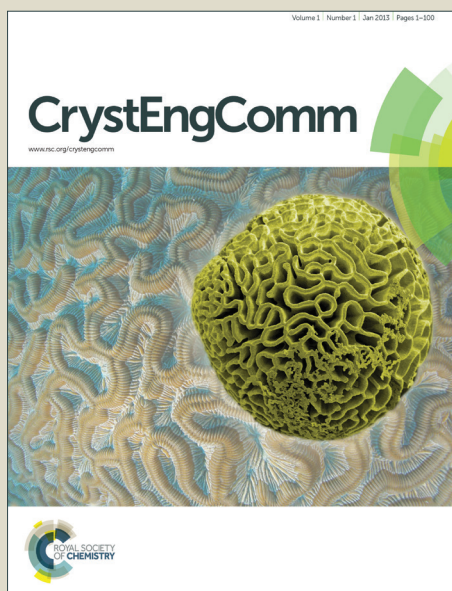


CrystEngComm

Accepted Manuscript



This is an *Accepted Manuscript*, which has been through the Royal Society of Chemistry peer review process and has been accepted for publication.

Accepted Manuscripts are published online shortly after acceptance, before technical editing, formatting and proof reading. Using this free service, authors can make their results available to the community, in citable form, before we publish the edited article. We will replace this *Accepted Manuscript* with the edited and formatted *Advance Article* as soon as it is available.

You can find more information about *Accepted Manuscripts* in the [Information for Authors](#).

Please note that technical editing may introduce minor changes to the text and/or graphics, which may alter content. The journal's standard [Terms & Conditions](#) and the [Ethical guidelines](#) still apply. In no event shall the Royal Society of Chemistry be held responsible for any errors or omissions in this *Accepted Manuscript* or any consequences arising from the use of any information it contains.

ARTICLE

The First 3D and The Trinuclear Cyano-bridged Fe^{III}–Fe^{III}(CN)₆ Complexes: Structure and Magnetic Characterizations

Cite this: DOI: 10.1039/x0xx00000x

Elif Gungor,^a Yasemin Yahsi,^a Hulya Kara,^{a,*} Andrea Caneschi^{b,*}Received 00th January 2015,
Accepted 00th January 2015

DOI: 10.1039/x0xx00000x

www.rsc.org/

[Fe(SB)(H₂O)]ClO₄ and [NEt₄]₃[Fe(CN)₆] react in methanol to give a *cis* cyano-bridged assembly, 3D [NEt₄][Fe(5-CIL1)]₂Fe(CN)₆, [5-CIL1H₂ = N,N'-bis(5-chlorosalicylideno)-2,2-dimethyl-1,3-diaminopropane], **1**, and a *trans* cyano-bridged trinuclear complex [NEt₄][Fe(5-CIL2)(MeOH)]₂Fe(CN)₆, [5-CIL2H₂ = N,N'-bis(5-chlorosalicylideno)-1,2-diaminopropane], **2**, depending on the Schiff-base used. Complexes **1** and **2** have been characterized by X-ray analyses and magnetic measurements. The four CN⁻ in the equatorial plane of the [Fe(CN)₆]³⁻ moiety bridge four Fe ions each in the *cis* position, which results in a 3D neutral layered structure giving a [-Fe-NC-Fe-CN-Fe-] linkage for **1**. The two CN⁻ in the equatorial plane of the [Fe(CN)₆]³⁻ moiety bridge two Fe ions, in the *trans* position, which results in a hydrogen bonded 2D neutral layered structure for **2**. Magnetic studies reveal that complex **1** exhibit weak intralayer ferromagnetic coupling, while complex **2** displays transition to a 3D ferromagnetic order between low-spin Fe(III) and high-spin Fe(III) through the cyanide bridges. Complex **2** further displays frequency dependent of alternating current (ac) magnetic susceptibility.

Introduction

In recent years, there has been considerable interest in the rational design and synthesis of molecule-based magnetic materials, which can originate many peculiar systems such as room-temperature magnet,¹ spin-crossover materials,² single-molecule magnets (SMMs),³ single-chain magnets (SCMs)⁴ and photomagnetic material⁵. In this framework the cyano-bridged magnetic complexes have been thoroughly investigated because of their interesting magnetic properties.⁶ In particular, self-assembled complexes of [M^{III}(SB)]⁺ (SB = Schiff-base ligands) and hexacyanometalates [M(CN)₆]³⁻ (M = Fe(III), Cr(III), Mn(III)) or octacyanometalates [M(CN)₈]⁴⁻ (M=Mo(IV), Mo(V), W(IV), W(V)) have been widely studied.⁷⁻¹³ Some of them exhibit SMM or SCM properties induced by the relevant magnetic anisotropy of Mn(III) and low-spin Fe(III).^{7b,7d,10-12} Following this research line we recently reported the synthesis, crystal structure and magnetic properties of two *cis* cyano-bridged assemblies with 3D structures, and a *trans* cyano-bridged trinuclear Mn^{III}–Fe^{III}–Mn^{III} cluster which behaved as a SMM at low temperature.¹⁰

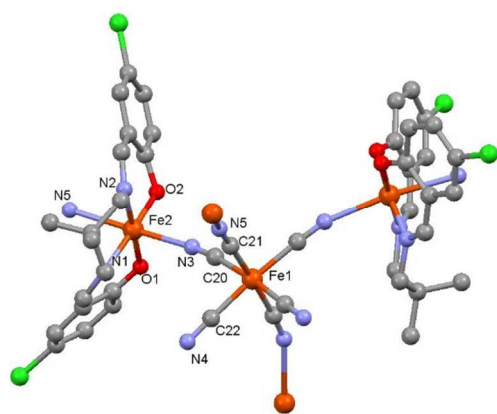
On the other hand to the best of our knowledge, only two examples obtained starting by [Fe(CN)₆]³⁻, and [Fe^{III}(SB)]⁺ building blocks have been characterized structurally and magnetically. These are [(NEt₄){Fe(salen)}₂{Fe(CN)₆}]_n and [{Fe(salen)}₃{Fe(CN)₆}(MeOH)₂].3nH₂O, salen=N, N'-ethylenebis(salicylideneiminato) dianion], displaying an extended 2D structure and exhibits a meta-magnetic behaviour.¹⁴

In an effort to enlarge the library of such complexes, we report here in the synthesis, crystal structure and magnetic properties of two complexes, *cis* cyano-bridged assembly with 3D structure, [NEt₄][Fe(5-CIL1)]₂Fe(CN)₆, **1**, [5-CIL1H₂ = N,N'-bis(5-chlorosalicylideno)-2,2-dimethyl-1,3-diaminopropane)] and a *trans* cyano-bridged trinuclear complex [NEt₄][Fe(5-CIL2)(MeOH)]₂Fe(CN)₆, **2**, [5-CIL2H₂ = N,N'-bis(5-chlorosalicylideno)-1,2-diaminopropane)]. Complex **1** is the first case of *cis* cyanide-bridged with 3D architecture constructed by the Fe-CN-Fe-NC-Fe linkages.

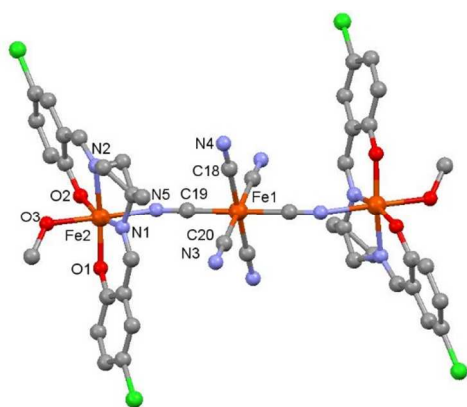
Results and discussion

Structural descriptions

The crystal data and structure refinement details for complexes **1** and **2** are listed in Table 1. Selected bond lengths and angles are summarized in Table 2. Representative structural diagrams of complexes **1** and **2** are shown in Fig. 1, while packing diagrams are given in Fig. 2, Fig.3, Fig.4 and Fig. 5. It is evident that, even if the same 1:1 stoichiometric conditions have been used to obtain **1** and **2**, complex **1** give rise to 3D coordination network, characterized by a layered structure while complex **2** is built up by isolated molecule interacting through an hydrogen bonded 2D structure. The final structural arrangement of the assembled complex is thus strongly dependent on the packing effects, which is tuned by the employed type of Schiff Base ligand and counterions.



(a)



(b)

Fig. 1 The molecular structure of **1** (a) and **2** (b). The hydrogen atoms, $[\text{NEt}_4]^+$ and solvent molecules have been omitted for clarity.

Table 1. Crystal data and structure refinement complex **1** and **2**.

	1	2
Chemical Formula	$\text{Fe}_3\text{C}_{52}\text{H}_{56}\text{Cl}_4\text{N}_{11}\text{O}_4$	$\text{Fe}_3\text{C}_{50}\text{H}_{54}\text{Cl}_4\text{N}_{11}\text{O}_6$
M_w	1208.43	1214.39
Crystal system	Trigonal	Monoclinic
Space group	$P3(1)21$	$P2_1/c$
Unit cell dimensions	a = 16.3482(3) Å b = 16.3482(3) Å c = 19.5011(6) Å $\alpha = 90^\circ$ $\beta = 90^\circ$ $\gamma = 120^\circ$	a = 12.470(3) Å b = 15.441(3) Å c = 15.443(3) Å $\alpha = 90^\circ$ $\beta = 114.56(3)^\circ$ $\gamma = 90^\circ$
V / Å ³	4513.7(5)	2704.5(14)
T / K	293	100(2)
Z	3	2
$\rho_{\text{calc}} / \text{g cm}^{-3}$	1.334	1.491
μ / mm^{-1}	0.941	1.050
Reflections collected	14656	18660
Independent reflections	4881	3604
$R_1 [I > 2\sigma(I)]$	0.0563	0.0720
WR2	0.1353	0.1918
Flack	0.062(19)	

Structural Analysis of **1**

Complex **1** crystallizes in a trigonal lattice, and the molecular moieties consist of one $[\text{Fe}^{\text{III}}(\text{CN})_6]^{3-}$ anion, two $[\text{Fe}^{\text{III}}(5\text{-CIL1})]^+$, one $[\text{NEt}_4]^+$ cations. The asymmetric unit contains one-half of a trinuclear (Fe-CN-Fe-NC-Fe) unit as well as half $[\text{NEt}_4]^+$ cation, since the central Fe(1) ion lie on a 2-fold rotation axis. The $[\text{Fe}(\text{CN})_6]^{3-}$ fragment exhibits a coordination close to octahedral in complex **1**: Fe(1)–C bond lengths are in the range 1.939(5)–1.978(4) Å and Fe(1)–C≡N bond angles in the range 174.0(4)–176.8(5)°. All these parameters are consistent for a low-spin Fe(III), as expected for a cyanide derivative.^{10,14}

The Fe(2) ion assumes a tetragonally elongated coordination geometry, in which the equatorial sites are occupied by N_2O_2 donor atoms of the quadridentate Schiff-base ligand with Fe(2)–O and Fe(2)–N distances of 1.872(3)–1.892(3), 2.011(4)–2.026(4) Å, respectively; and the axial positions are occupied by two nitrogen atoms from CN[−] groups with Fe(2)–N_{cyno} distance 2.360(4)–2.414(4) Å, thus the Jahn–Teller axis lies along the N_{cyno}–Fe(2)–N_{cyno} axis. The bridging Fe(2)–N≡C bond angles lie in the range 156.7(4)–165.6(4)°. These data are comparable with those previously reported for strictly related complexes.^{10,14}

For **1** each $[\text{Fe}(\text{CN})_6]^{3-}$ anion coordinates with four $[\text{Fe}(5\text{-CIL1})]^+$ cations via four equatorial C≡N groups each in the *cis* positions, which results in a 3D neutral layered structure consisting of $[-\text{Fe}(\text{III})\text{-CN-Fe}(\text{III})\text{-NC-}]$ units (Scheme S1). The layers are connected by $\text{Fe}(1)_6\text{Fe}(2)_6$ closed structures connected at each Fe(III) centers. It is interesting to note that different layered structure are observed in the *ac*-plane, stacked orthogonally to the *b*-axis (Fig. 2), and in the *bc*-plane, stacked orthogonally to the *a*-axis for **1** (Fig. S3). $[\text{NEt}_4]^+$ and solvent molecules of crystallization fill the interlayer spaces, while the building up of the pattern is assured by the availability of two nitrogen per each $[\text{Fe}(5\text{-CIL1})]^+$ fragment. Finally, we note that the interconnection of zig-zag chains of the $\text{Fe}(\text{CN})_6\text{Fe}_2$ unit results in an alternate hexagonal/trigonal pattern along the *c*-axis, as shown in Fig. 3.

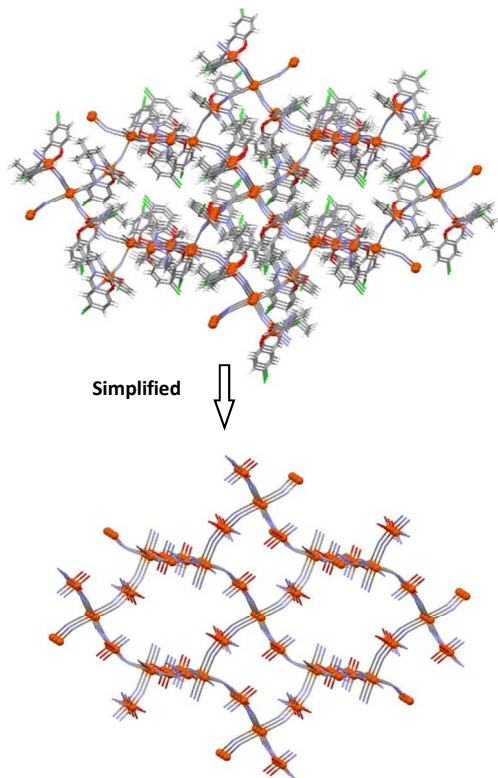


Fig. 2A A three-dimensional network structure in the *ac*-plane and its simplified network topology of **1** (only considering Fe (orange) atoms as nodes). $[\text{NEt}_4]^+$ molecule have been omitted for clarity.

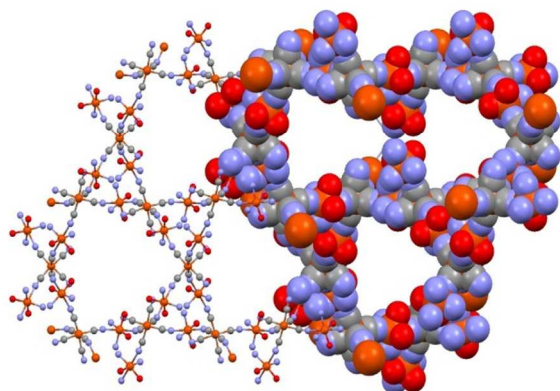


Fig. 3 View of the hexagonal/trigonal pattern of the $\text{Fe}(\text{CN})_6\text{Fe}_2$ skeleton of **1** along the *c* axis. The hydrogen atoms and the carbon atoms of the Schiff base ligands and $[\text{NEt}_4]^+$ molecule are omitted for clarity.

Structural Analysis of 2

In contrast to **1**, the structure of complex **2** consists of the trinuclear $\{[(\text{MeOH})\text{Fe}(\text{5-CIL2})_2\text{Fe}(\text{CN})_6]^-$ anion and $[\text{NEt}_4]^+$ cation. Since the space group is $P2_1/c$ and the unit cell contains two trinuclear molecular units, the asymmetric unit is one-half of a trinuclear unit, the $\text{Fe}(1)^{\text{III}}$ ion occupying an inversion center. The two CN^- groups in trans positions of the $[\text{Fe}(\text{CN})_6]^{3-}$ moiety bridge two Fe^{III} ions, giving a repeating motif $\text{Fe}-\text{NC}-\text{Fe}-\text{CN}-\text{Fe}$. The Fe^{III} center show coordination parameters in agreement with previous reports for $[\text{Fe}(\text{CN})_6]^{3-}$.

The $\text{Fe}(2)$ site exhibits an octahedral distorted geometry, in which the equatorial sites occupied by N_2O_2 donor atoms of the quadridentate Schiff-base ligand. $\text{Fe}-\text{O}$ distances of the $[\text{Fe}(\text{5-CIL2})]^+$ cations are $\text{Fe}(2)-\text{O}(1)=1.891(3)$ Å and $\text{Fe}(2)-\text{O}(2)=1.902(4)$ Å while $\text{Fe}-\text{N}$ distances are $\text{Fe}(2)-\text{N}(1)=2.107(5)$ Å and $\text{Fe}(2)-\text{N}(2)=2.113(5)$ Å. The two axial positions are occupied by a cyanide group of $[\text{Fe}(\text{CN})_6]^{2-}$ ($\text{Fe}(2)-\text{N}(5)=2.111(4)$ Å) and by a methanol molecule ($\text{Fe}(2)-\text{O}(3)=2.133(4)$ Å). These data are comparable with those of related complexes previously reported.^{10,14} The trinuclear units are held together by a hydrogen bonding network established by the $\text{Fe}(2)$ -bonded methanol ($\text{O}3\dots\text{N}4 = 2.696$ Å), which leads to a two dimensional extended structure (Scheme S2, Fig. 4).

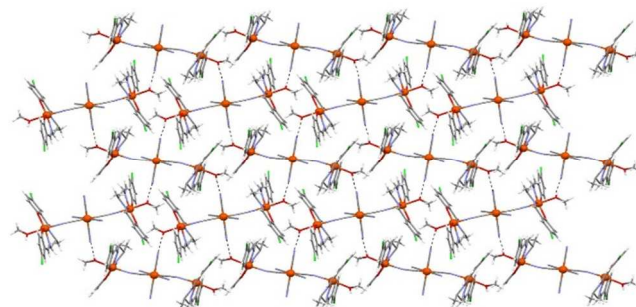


Fig. 4 A two-dimensional network structure formed by hydrogen bonds in the *bc*-plane of **2**. $[\text{NEt}_4]^+$ molecules have been omitted for clarity.

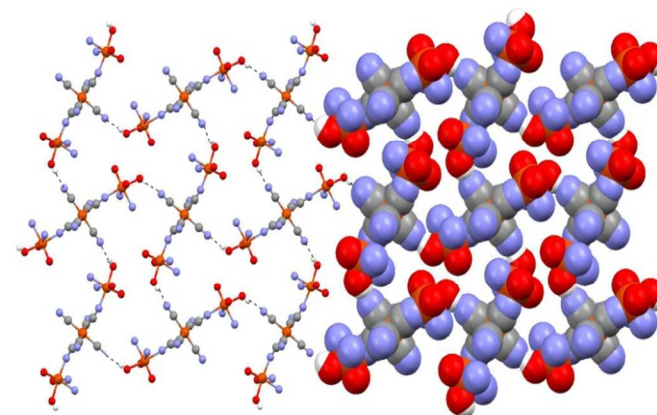


Fig. 5 View of the 2D pattern of the $\text{Fe}(\text{CN})_6\text{Fe}_2$ skeleton of **2** along the *a* axis. The hydrogen atoms, solvent molecules, and carbon atoms of the Schiff base ligands are omitted for clarity.

Finally, before proceeding to the magnetic characterization, we note that X-ray powder patterns for bulk microcrystalline samples of each of **1** and **2** were consistent with the exclusive presence of the phase identified in the single crystal experiment (Fig. S1–S2).

Magnetic Properties of Complexes 1

The magnetic properties of complex **1** are reported in Fig. 6, in the form of χT vs *T*. The χT value per $\text{Fe}^{\text{II}}_2\text{Fe}^{\text{III}}$ unit at room temperature is 11.2 emu K mol⁻¹, which is higher than the spin-only value of 9.2 emu K mol⁻¹ expected for two $S=5/2$ and one $S=1/2$ independent spins. This discrepancy might be due to the relatively large orbital contribution of low spin $\text{Fe}(\text{III})$ which features a $^2T_{2g}$ ground state. On lowering the temperature, the χT value (measured at

1 KOe) slowly decrease until 30 K, then increases gradually in the 30–3 K range, and finally drops to 12.9 emu K mol⁻¹ at 1.8 K, respectively. The decrease observed in the high temperature range may be attributed either to ligand field effects of the low spin Fe(III) or to weak antiferromagnetic interaction. However, the high field value of the magnetization observed at low temperature (11.3 μ_B) clearly excludes an antiferromagnetic interaction to be dominant. The increase in χT observed in the 30–3 K range should be attributed, in this framework, to the presence of weak intralayer ferromagnetic coupling in **1**, whereas the lowest temperature decrease might be due to interlayer weak antiferromagnetic coupling and/or anisotropy effects.

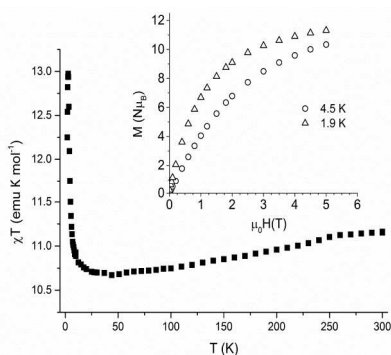


Fig. 6 Temperature dependence of χT per Fe₃ unit for **1**; the inset shows the isothermal magnetization curves measured two different temperatures.

It is interesting to note that the magnetic property of complex **1** is different from that of their congeners reported in literature¹⁴ (see

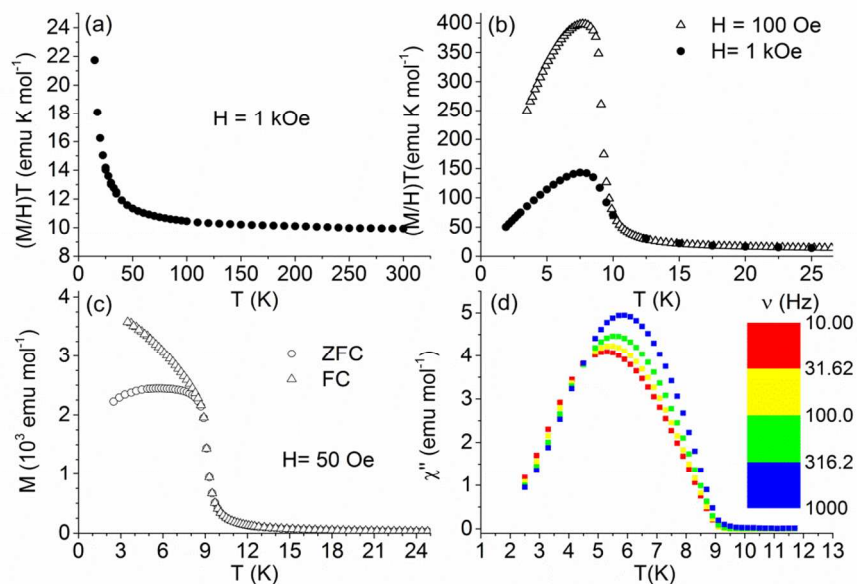


Fig. 7 (a) Temperature dependence of the (M/H)T product of **2** measured at 1 KOe, detail of the higher temperature range (b) Temperature dependence of the (M/H)T product of **2** measured at 1 KOe and 100 Oe, detail of the low temperature range (c) ZFC/FC curves of **2**, measured at 50 Oe (d) Temperature dependence of the imaginary part of the susceptibility of **2** at different frequencies and in zero static field.

Experimental

General Procedures and Materials

Table S1): in particular, no evident sign of ordering could be observed. Only a very small contribution of χ'' (with a value of about 1% of the χ' one) is observable at low temperature (see Fig. S4). This is tentatively attributed to the different structural features induced by different substituents introduced in the Schiff base moieties, the counterion and the crystallization solvent.

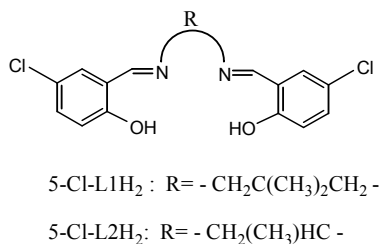
Magnetic Properties of Complex 2

The magnetic properties of complex **2** are reported in Fig. 7. The χT value per Fe^{III}₂Fe^{III} unit at room temperature, 9.92 emu K mol⁻¹ is only slightly higher than the spin-only value of 9.50 emu K mol⁻¹, expected for the magnetically dilute spin system ($S_{\text{Fe}(\text{hs})}$, $S_{\text{Fe}(\text{ls})}$, $S_{\text{Fe}(\text{hs})} = (5/2, 1/2, 5/2)$ assuming $g = 2.0$).

Lowering the temperature, the χT slightly increases down to 20 K, then abruptly peaks at 140 emu K mol⁻¹ at 7.5 K, to decrease sharply to 50 emu K mol⁻¹ at 1.9 K. Interestingly the observed maximum value is strongly field dependent (Fig. 7b), clearly suggesting the onset of long range ordering. This was confirmed by ZFC/FC magnetization curves, which evidences a transition temperature of 9.1 K (Fig. 7c). The observation of long range order clearly points to a major role of the hydrogen bond network in transmitting relevant interactions between adjacent trinuclear units, which are ferromagnetically coupled. Ac susceptibility measurements further confirmed the long range order (Fig. 7d). It is however interesting to note that, below the transition temperature, some frequency dependence of the imaginary part of the susceptibility is observed.

All chemicals and solvents used for synthesis were reagent grade. The quadridentate Schiff base ligands, 5-CIL1H₂ (N,N'-bis(5-Chloro-2-hydroxybenzylidene)-2,2,-dimethylpropane-1,3,-diamine) and 5-CIL2H₂ (N,N'-bis(5-Chloro-2-hydroxybenzylidene)-1,2-

propane-diamine) were synthesized by mixing the corresponding chlorosalicylaldehyde and 2,2-dimethyl-1,3-diaminopropane or 1,2-diaminopropane in a 2:1 mole ratio in ethanol according to the literature.¹⁵ $[\text{NEt}_4]_3[\text{Fe}(\text{CN})_6]$ was prepared according to the literature.¹⁶ Since the hexacyanometalate ion has a tendency to decompose on heating or irradiation, the syntheses of the complexes were performed at room temperature and the crystallization was performed in a dark room. Diagram of the ligands are reported in Scheme 1.



Scheme 1. Schematic diagram of the ligands

Caution: Perchlorate salts are potentially explosive and should only be handled in small quantities.

Preparation of Iron (III) Schiff Base Complex

The iron(III) complexes were prepared by mixing FeCl_3 and the appropriate Schiff base ligand in methanol in a molar ratio of 1:1 according to the method reported previously.¹⁵

Preparation of 1 and 2

To a solution of appropriate Iron(III) Schiff base complexes (0.1 mmol) in methanol was added a solution of $[\text{NEt}_4]_3[\text{Fe}(\text{CN})_6]$ (0.1 mmol) in methanol at a room temperature. The resulting solution was allowed to stand for one week at room temperature in a dark room, and the single crystals precipitated and were collected by suction filtration, washed with a minimum volume of methanol, and dried *in vacuo*.

Complex 1: Yield: 60%, Anal. Calcd. for $\text{Fe}_3\text{C}_{54}\text{H}_{68}\text{Cl}_4\text{N}_{11}\text{O}_8$: C, 49.57; H, 5.24; N, 11.77. Found: C, 50.25; H, 5.38; N, 11.60%. IR ($\text{KBr}/\text{cm}^{-1}$): $\nu(\text{C}\equiv\text{N})$ 2025, $\nu(\text{C}=\text{N})$ 1611.

Complex 2: Yield: 65%, Anal. Calcd. for $\text{Fe}_3\text{C}_{50}\text{H}_{54}\text{Cl}_4\text{N}_{11}\text{O}_6$: C, 49.45; H, 4.48; N, 12.69. Found: C, 50.09; H, 4.90; N, 12.81%. IR ($\text{KBr}/\text{cm}^{-1}$): $\nu(\text{C}\equiv\text{N})$ 2100, $\nu(\text{C}=\text{N})$ 1610.

Physical measurements

Elemental analyses (C, H, and N) were carried out by standard methods. FT-IR spectra were measured with a Perkin-Elmer Model Bx 1600 instrument with the samples as KBr pellets in the 4000 – 400 cm^{-1} range. DC Magnetic measurements were performed using a QD Squid magnetometer with applied field of 0.1 T, except when otherwise stated. To avoid possible orientation effects, microcrystalline powders were pressed in pellets. The data were

corrected for sample holder contribution and diamagnetism of the sample using Pascal constants. Ac susceptibility measurements were performed with the same instrument in the range 10-1000 Hz, without static applied field, and an amplitude of the oscillating field of 3 Oe.

Crystallography

Diffraction measurements were made on a Bruker ApexII kappa CCD diffractometer using graphite monochromated $\text{Mo-K}\alpha$ radiation ($\lambda = 0.71073 \text{ \AA}$) at 100 K for **1** and **2**. The intensity data were integrated using the APEXII program.¹⁷ Absorption corrections were applied based on equivalent reflections using SADABS.¹⁸ The structures were solved by direct methods and refined using full-matrix least-squares against F^2 using SHELXL.¹⁹ All non-hydrogen atoms were assigned anisotropic displacement parameters and refined without positional constraints. Hydrogen atoms were included in idealized positions with isotropic displacement parameters constrained to 1.5 times the U_{equiv} of their attached carbon atoms for methyl hydrogens, and 1.2 times the U_{equiv} of their attached carbon atoms for all others. One water and one methanol molecules in the crystal lattice appear to be highly disordered, and it was difficult to model reliably their positions and distribution. Therefore, the SQUEEZE function of PLATON²⁰ was used to eliminate the contribution of the electron density in the solvent region from the intensity data, and the solvent free model was employed for the final refinement. The solvent molecules and their hydrogen atoms weren't included in the total atomic formula and they are not included in the list of atoms. Chemical analysis for this complex suggests the occurrence of one lattice water and methanol molecules. A possible disorder in 1,2-diaminopropane portion of the ligand and the balance anion $[\text{NEt}_4]^+$ molecule for **2** has been considered. Carbon atoms in $[\text{NEt}_4]^+$ molecule were refined isotropically due to its high thermal motion. The absolute structure was determined on the basis of the Flack parameter²¹ $x = 0.062(10)$ for **1**. A Flack parameter value close to 0 is indicative of a non-centrosymmetric structure.

Powder X-ray measurements were performed using $\text{Cu-K}\alpha$ radiation ($\lambda = 1.5418 \text{ \AA}$) on a Bruker-AXS D8-Advance diffractometer equipped with a secondary monochromator. The data were collected in the range $5^\circ < 2\theta < 60^\circ$ in θ - θ mode with a step time of ns ($5 \text{ s} < n < 10 \text{ s}$) and step width of 0.02° .

Table 2. Some selected bond lengths [\AA] and angles [$^\circ$] for complex **1** and **2**.

	1	2
Fe2–N _{salen}	2.011(4)–2.026(4)	2.107(5)–2.113(5)
Fe2–O	1.872(3)–1.892(3)	1.891(3)–1.902(4)
Fe2–O _{metoh}		2.133(4)
Fe2–N _{evano}	2.360(4)–2.414(4)	2.111(4)
Fe1–C	1.939(5)–1.978(4)	1.932(5)–1.956(6)
Fe2–N \equiv C	156.7(4)–165.6(4)	152.9(5)
Fe1–C \equiv N	174.0(4)–176.8(5)	175.3(5)–179.4(4)
Fe1–Fe2 ^a	5.418	5.025
Fe2–Fe2 ^b	9.208	10.050

^aAdjacent intermetallic separations through the cyanide bridges. ^bInterchain metal–metal separations.

Conclusions

Two heterobimetallic *cis* cyano-bridged 3D and a *trans* cyano-bridged trinuclear clusters have been designed and synthesized using $[\text{NEt}_4]_3[\text{Fe}(\text{CN})_6]$ and two manganese(III) compounds containing

Schiff base ligands as building blocks. The significant difference in the structural features between **1** and **2**, are reflected in the different magnetic behaviour of these complexes. In **1**, each $[\text{Fe}(\text{CN})_6]^{3-}$ anion coordinates with four $[\text{Fe}(5\text{-C1L1})]^+$ cations *via* four equatorial C≡N groups each in the *cis* positions, which results in a 3D neutral layered structure consisting of $[-\text{Fe}-\text{NC}-\text{Fe}-\text{CN}-\text{Fe}-]$ linkage. In **2**, the two CN⁻ groups in trans positions of the $[\text{Fe}(\text{CN})_6]^{3-}$ moiety bridge two Fe^{III} ions, giving a repeating motif Fe–NC–Fe–CN–Fe. The trinuclear units are held together by a hydrogen bonding network, which leads to a 2D neutral layered structure of **2**. The magnetic data indicate that complexes **1** exhibit weak intralayer ferromagnetic coupling between the adjacent Fe^{III} and Mn^{III} ions through cyanide-bridges while complex **2** displays transition to a 3D ferromagnetic order between low-spin Fe(III) and high-spin Fe(III) through the cyanide bridges.

Acknowledgements

The authors are grateful to the Scientific and Technological Research Council of Turkey (TUBITAK) (grant number TBAG-108T431) for the financial support. Dr. Kara would like to thank TUBITAK for NATO-B1 and the Royal Society short visit fellowship for financial support and Prof. A. Guy Orpen (School of Chemistry, University of Bristol, UK) for his hospitality. The authors are also very grateful to Dr. Mairi F. Haddow (The School of Chemistry, University of Bristol) for the X-ray measurements and Dr. Lorenzo Sorace (Department of Chemistry, University of Florence) for the SQUID measurements and helpful suggestions.

Notes and references

^aBalikesirUniv, Fac Art &Sci, DeptPhys, TR-10145 Balikesir, Turkey
Email:hkara@balikesir.edu.tr

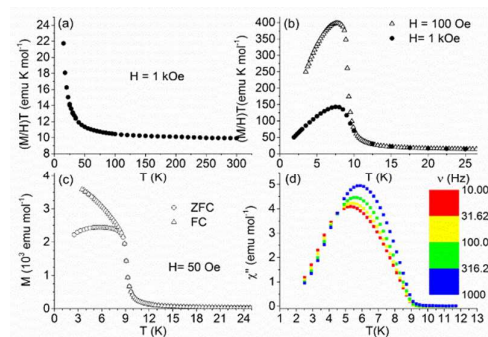
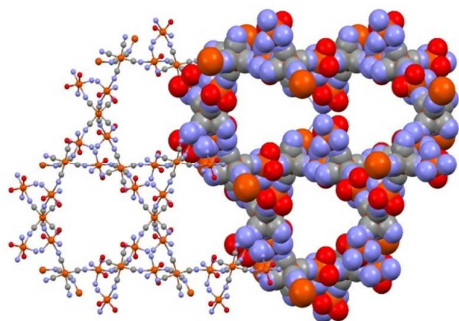
^bDipartimento di Chimica “U. Schiff” and UdR INSTM, Università di Firenze, Sesto Fiorentino (FI), Italy.
Email: andrea.caneschi@unifi.it

Electronic Supplementary Information (ESI) available: [Schematic diagram of **1** and **2**, powder XRD data of **1** and **2**, 3D packing structure of **1**, and the magnetic data for **1** and **2**. CCDC data1041739 and 1041740, these data can be obtained free of charge from The Cambridge Crystallographic Data Centre via www.ccdc.cam.ac.uk/data_request/cif. See DOI: 10.1039/b000000x/

- [1] (a) J. M. Manriquez, G. T. Yee, R. S. McLean, A. J. Epstein, J. S. Miller, *Science*, 1991, **252**, 1415; (b) S. Ferlay, T. Mallah, R. Ouahes, P. Veillet, M. Verdaguer, *Nature*, 1995, **378**, 701.
- [2] (a) M. Clemente-Leon, E. Coronado, M. Lopez-Jorda, G. M. Espallargas, A. Soriano-Portillo, J. C. Waerenborgh, *Chem. Eur. J.*, 2010, **16**, 2207; (b) S. Ohkoshi, K. Imoto, Y. Tsunobuchi, S. Takano, H. Tokoro, *Nat. Chem.*, 2011, **3**, 564.
- [3] (a) R. Sessoli, D. Gatteschi, A. Caneschi, M. A. Novak, *Nature*, 1993, **365**, 141; (b) L. Thomas, F. Lioni, R. Ballou, D. Gatteschi, R. Sessoli, B. Barbara, *Nature*, 1996, **383**, 145; (c) J. R. Friedman, M. P. Sarachik, J. Tejada, R. Ziolo, *Phys. Rev. Lett.*, 1996, **76**, 3830; (d) A. D. Katsenis, R. Inglis, A. Prescimone, E. K. Brechin and G. S. Papaefstathiou, *CrystEngComm*, 2012, **14**, 1216; (e) A. Perivolaris, A. M. Fidelli, R. Inglis, V. G. Kessler, A. M. Z. Slawin, E. K. Brechin, G. S. Papaefstathiou, *J. Coord. Chem.*, 2014, **67**, 3972; (f) D. Gatteschi, R. Sessoli, *Angew. Chem. Int. Ed.*, 2003, **42**, 268; (g) M. Mannini, F. Pineider, P. Sainctavit, C. Danieli, E. Otero, C. Sciancalepore, A. M. Talarico, M. A. Arrio, A. Cornia, D. Gatteschi, R. Sessoli, *Nature Materials*, 2009, **8**, 194; (h) M. Mannini, F. Pineider, C. Danieli, F. Totti, L. Sorace, E. P. Sainctavit, M. A. Arrio, Otero, L. Joly, J. C. Cezar, A. Cornia, R. Sessoli, *Nature*, 2010, **468**, 417.
- [4] (a) A. Caneschi, D. Gatteschi, N. Lalioti, C. Sangregorio, R. Sessoli, G. Venturi, A. Vindigni, A. Rettori, M. G. Pini, M. A. Novak, *Angew. Chem.*, 2001, **113**, 1810; *Angew. Chem. Int. Ed.*, 2001, **40**, 1760; (b) R. Clerac, H. Miyasaka, M. Yamashita, C. Coulon, *J. Am. Chem. Soc.*, 2002, **124**, 12837; (c) K. Bernot, J. Luzon, R. Sessoli, A. Vindigni, J. Thion, S. Richeter, D. Leclercq, J. Larionova, A. van der Lee, *J. Am. Chem. Soc.*, 2008, **130**, 1619; (d) R. Lescouze, J. Vaissermann, C. Ruiz-Perez, F. Lloret, R. Carrasco, M. Julve, M. Verdaguer, Y. Dromzee, D. Gatteschi, W. Wernsdorfer, *Angew. Chem.*, 2003, **115**, 1521; *Angew. Chem. Int. Ed.* 2003, **42**, 1483; (e) E. Pardo, R. Ruiz-Garcia, F. Lloret, J. Faus, M. Julve, Y. Journaux, F. Delgado, C. Ruiz-Perez, *Adv. Mater.*, 2004, **16**, 1597; (f) T. F. Liu, D. Fu, S. Gao, Y. Z. Zhang, H. L. Sun, G. Su, Y. J. Liu, *J. Am. Chem. Soc.*, 2003, **125**, 13976; (g) T. Kajiwara, M. Nakano, Y. Kaneko, S. Takaishi, T. Ito, M. Yamashita, A. Igashira-Kamiyama, H. Nojiri, Y. Ono, N. Kojima, *J. Am. Chem. Soc.*, 2005, **127**, 10150; (h) Y. L. Bai, J. Tao, W. Wernsdorfer, O. Sato, R. B. Huang, L. S. Zheng, *J. Am. Chem. Soc.*, 2006, **128**, 16428.
- [5] (a) S. I. Ohkoshi, H. Tokoro, *Acc. Chem. Res.*, 2012, **45**, 1749; (b) L. Bogani, L. Cavigli, M. Gurioli, R. L. Novak, M. Mannini, A. Caneschi, F. Pineider, R. Sessoli, M. Clemente-Leon, E. Coronado, A. Cornia, D. Gatteschi, *Adv. Mater.*, 2007, **19**, 3906; (c) C. D. Fernandez, G. Mattei, E. Paz, R. L. Novak, L. Cavigli, L. Bogani, F. J. Palomares, P. Mazzoldi, A. Caneschi, *Nanotech.*, 2010, **21**, 1259; (c) R. Moroni, R. Buzio, A. Chincarini, U. Valbusa, F. B. de Mongeot, L. Bogani, A. Caneschi, R. Sessoli, L. Cavigli, M. Gurioli, *J. Mater. Chem.*, 2008, **18**, 109.
- [6] (a) C. Yang, Q. L. Wang, J. Qi, Y. Ma, S. P. Yan, G. M. Yang, P. Cheng, and D. Z. Liao, *Inorg. Chem.*, 2011, **50**, 4006; (b) L. Sorace, C. Sangregorio, A. Figuerola, C. Benelli and D. Gatteschi, *Chem. Eur. J.*, 2009, **15**, 1377; (c) Y. Q. Zhang, C. L. Luo, X. B. Wu, B. W. Wang, S. Gao, *Inorg. Chem.*, 2014, **53**, 3503; (d) Y. Q. Zhang, C. L. Luo, *Inorg. Chem.*, 2009, **48**, 10486; (d) L. Chen, J. Wang, J. M. Wei, W. Wernsdorfer, X. T. Chen, Y. Q. Zhang, Y. Song, Z. L. Xue, *J. Am. Chem. Soc.*, 2014, **136**, 12213; (e) M. X. Yao, Q. Zheng, X. M. Cai, Y. Z. Li, Y. Song, J. L. Zuo, *Inorg. Chem.*, 2012, **51**, 2140; (f) H. B. Zhou, J. Wang, H. S. Wang, Y. L. Xu, X. J. Song, Y. Song, X. Z. You, *Inorg. Chem.*, 2011, **50**, 6868; (g) C. C. Zhao, W. W. Ni, J. Tao, A. L. Cui and H. Z. Kou, *CrystEngComm*, 2009, **11**, 632; (h) D. P. Zhang, H. L. Wang, L. J. Tian, H. Z. Kou, J. Z. Jiang, Z. H. Ni, *Cryst. Growth Des.*, 2009, **9**, 3989; (i) G. L. Li, L. F. Zhang, Z. H. Ni, H. Z. Kou, A. L. Cui, *Bull. Korean Chem. Soc.*, 2012, **33**, 1675; (j) G. L. Li, W. Q. Cheng, L. F. Zhang, Z. H. Ni, M. M. Yu, H. Z. Kou, *Trans. Met. Chem.*, 2012, **37**, 469; (k) J. E. Jee, C. H. Kwak, *Inorg. Chem. Commun.*, 2013, **33**, 95; (l) H. Kim, J. Y. Lee, S. G. Kang, C. H. Kwak, *Bull. Korean Chem. Soc.*, 2014, **35**, 305.
- [7] (a) H. Miyasaka, H. Ieda, N. Matsumoto, N. Re, R. Crescenzi and C. Floriani, *Inorg. Chem.*, 1998, **37**, 255; (b) H. J. Choi, J. J. Sokol and J. R. Long, *Inorg. Chem.*, 2004, **43**, 1606; (c) H. Miyasaka, N. Matsumoto, H. Okawa, N. Re, E. Gallo and C. Floriani, *J. Am. Chem. Soc.*, 1996, **118**, 981; (d) M. Ferbinteanu, H. Miyasaka, W. Wernsdorfer, K. Nakata, K. Sugiura, M. Yamashita, C. Coulon and R. Clerac, *J. Am. Chem. Soc.*, 2005, **127**, 3090; (e) N. Re, E. Gallo, C. Floriani, H. Miyasaka and N. Matsumoto, *Inorg. Chem.*, 1996, **35**, 6004.
- [8] (a) H. H. Ko, J. H. Lim, H. S. Yoo, J. S. Kang, H. C. Kim, E. K. Koh, C. S. Hong, *Dalton Trans.*, 2007, 2070; (b) P. Przychodzen, K. Lewinski, M. Balanda, R. Pelka, M. Rams, T. Wasiutynski, C. Guyard-Duhayon, B. Sieklucka, *Inorg. Chem.*, 2004, **43**, 2967; (c) P. Przychodzen, M. Rams, C. Guyard-Duhayon, B. Sieklucka, *Inorg. Chem. Commun.*, 2005, **8**, 350.
- [9] (a) H. S. Yoo, H. H. Ko, D. W. Ryu, J. W. Lee, J. H. Yoon, W. R. Lee, H. C. Kim, E. K. Koh, C. S. Hong, *Inorg. Chem.*, 2009, **48**, 5617; (b) H. Z. Kou, Z. H. Ni, B. C. Zhou, R. J. Wang, *Inorg. Chem. Commun.*, 2004, **7**, 1150.
- [10] H. Kara, A. Azizoglu, A. Karaoglu, Y. Yahsi, E. Gungor, A. Caneschi and L. Sorace, *CrystEngComm*, 2012, **14**, 7320.

- [11] T. Glaser, M. Heidemeier, T. Weyhermuller, R. D. Hoffmann, H. Rupp and P. Muller, *Angew. Chem., Int. Ed.*, 2006, **45**, 6033.
- [12] H. Miyasaka, H. Takahashi, T. Madanbashi, K. I. Sugiura, R. Cl'eric and H. Nojiri, *Inorg. Chem.*, 2005, **44**, 5969.
- [13] H. Miyasaka, H. Okawa, A. Miyazaki and T. Enoki, *Inorg. Chem.*, 1998, **37**, 4878.
- [14] N. Re, R. Crescenzi, C. Floriani, H. Miyasaka, N. Matsumoto, *Inorg. Chem.*, 1998, **37**, 2717.
- [15] (a) Y. Yahsi, H. Kara, L. Sorace, O. Buyukgungor, *Inorg. Chem. Acta.*, 2011, **366**, 191; (b) A. Karakas, E. Donmez, H. Kara, A. Elmali, *J. Nonlinear Opt. Phys. Mater.*, 2007, **16**, 329.
- [16] P. K. Mascharak, *Inorg. Chem.*, 1986, **25**, 245.
- [17] Bruker-AXS SAINT V7.60A.
- [18] G. M. Sheldrick, SADABS V2008/1, University of Göttingen, Germany.
- [19] G. Sheldrick, *ActaCrystallogr., Sect. A: Found. Crystallogr.*, 2008, **A64**, 112.
- [20] A. L. Spek, *J. Appl. Crystallogr.*, 2003, **36**, 7.
- [21] H. D. Flack, *ActaCrystallogr.*, 1983, **A39**, 876.

Graphical Abstract

The First 3D and The Trinuclear Cyano-bridged Fe^{III}-Fe^{III}(CN)₆ Complexes: Structure and Magnetic CharacterizationsElif Gungor,^a Yasemin Yahsi,^a Hulya Kara,^{a,*} Andrea Caneschi^{b,*}

Crystal structure and magnetic properties of 3D *cis*-cyano-bridged and 2D *trans*-cyano-bridged trinuclear Fe^{III}-Fe^{III}(CN)₆ structures are reported.